December 1998

Density of Zeros on the Lee-Yang Circle Obtained from Magnetization Data of a Two-Dimensional Ising Ferromagnet

Christian Binek
University of Nebraska-Lincoln, cbinek@unl.edu

Density of Zeros on the Lee-Yang Circle Obtained from Magnetization Data of a Two-Dimensional Ising Ferromagnet

Ch. Binek

Angewandte Physik, Gerhard-Mercator-Universität Duisburg, D-47048 Duisburg, Germany

(Received 7 August 1998)

In order to provide experimental access to the statistical theory of Lee and Yang [Phys. Rev. **87**, 410 (1952)] the density function $g(\theta)$ of zeros on the Lee-Yang circle has been determined for the first time by analyzing isothermal magnetization data $m(H)$ of the Ising ferromagnet $FeCl_2$ in axial magnetic fields H at temperatures $34 \leq T \leq 99$ K. The validity of our approach is demonstrated by the perfect agreement of magnetic specific heat data as calculated from $g(\theta)$ and $m(H)$ via Maxwell's relation. Moreover, the correct in-plane exchange constant of $FeCl_2$ emerges from the series expansion of $m(H)$ involved in the analysis. [S0031-9007(98)08010-7]

PACS numbers: 75.10.Hk, 05.50.+q, 75.40.Cx

In 1952 Lee and Yang (LY) [1] pointed out that the distribution of the zeros of the partition function Z of an Ising ferromagnet reveals a remarkable symmetry in the complex fugacity plane. By virtue of their famous theorem they proved that in the case of an Ising ferromagnet, the zeros of Z are distributed on the unit circle $z = \exp(i\theta)$ in the complex $z = \exp(-2gS\mu_B\mu_0 H/k_B T)$ plane, where $gS\mu_B$ is the magnetic moment with Bohr's magneton μ_B, the spin quantum number S, and the Landé factor g, while H is the complex magnetic field, and T is the temperature. They conjectured that this symmetry has a simple and far reaching basis, which, however, still has to be discovered.

Up to now, little progress has been made within this fundamental field of statistical physics. Although it has been shown that the LY theorem is applicable to much wider classes of model systems [2,3], little is known about the distribution function $g(\theta)$ itself, which completely determines the thermodynamic behavior of the system. In particular, $g(\theta)$ has always been thought to be a purely theoretical quantity which is not accessible by experimental investigations. However, it is the aim of this Letter to demonstrate for the first time that $g(\theta)$ can be extracted from isothermal magnetization curves m vs H of Ising ferromagnets, provided that they are measured with high enough accuracy using, e.g., modern superconducting quantum interference device (SQUID) techniques.

From the theoretical point of view, there are two approaches to investigate $g(\theta)$. On the one hand, there are straightforward solutions of $Z(z) = 0$ for dimensions $D \geq 2$ which are, however, restricted to systems of a few interacting spins only [4–7]. On the other hand, the basic relation [1],

$$I(z) = 1 - 4z \int_0^\pi [g(\theta)(z - \cos\theta)/(z^2 - 2z\cos\theta + 1)]\, d\theta\,, \quad (1)$$

which correlates the normalized magnetization $I = m/m_s$ and $g(\theta)$, is used in order to approximate $g(\theta)$ from corresponding approximations of $I(z)$. Here m and m_s denote the magnetic moment and its saturation value. The coefficients of the high field series expansion

$$I(z) = 1 + 2\pi \sum_{n=1}^{\infty} g_n z^n \quad (2)$$

directly determine the coefficients $g_n = (2/\pi)\int_0^\pi g(\theta) \times \cos(n\theta)\, d\theta$, $n \geq 1$, of the Fourier cosine series of $g(\theta)$ [8]. Unfortunately, the poor convergence of the series (2) requires a huge number of expansion coefficients in order to satisfactorily represent $g(\theta)$. However, Kortman and Griffiths [10] pointed out that $g(\theta)$ may also be constructed, e.g., from quickly converging Padé approximants of $I(z)$ when using the relation,

$$g(\theta) = (1/2\pi) \lim_{r\to 1^-} \mathrm{Re}\, I[r\exp(i\theta)]\,. \quad (3)$$

This equation is easily verified by substitution of $z = r\exp(i\theta)$ into Eq. (2). As will be shown below, this ansatz turns out to be particularly useful for analyzing experimental data. Based on high field series expansions of $I(z)$ [11], Kortman and Griffiths computed the corresponding Padé approximants and calculated $g(\theta)$ for Ising ferromagnets on a 2D square and a 3D diamond lattice for $T \neq T_c$. In addition they investigated $g(\theta)$ for the mean-field model and the linear chain. Their solution of the latter problem was in good agreement with the rigorous analytical expression obtained previously by Lee and Yang [1].

In analogy to the procedure introduced by Kortman and Griffiths [10], we have determined $g(\theta)$ from experimental data m vs H by using, again, Eq. (3). To this end, the data sets are normalized with respect to the low temperature and high field saturation value m_s of the magnetic moment and subsequently best fitted to empirical functions of the type,

$$f(z) = [1 + n_1 z - (1 + n_1)z^2]/(1 + d_1 z + d_2 z^2)\,, \quad (4)$$

with appropriate parameters n_1, d_1, and d_2. The fitting functions take into account the limiting cases $f(z = 1) = 0$

 0031-9007/98/81(25)/5644(4)$15.00

and $f(z = 0) = 1$ of the normalized magnetization at $T > T_c$ in zero and infinite magnetic field, respectively. Once the fitting parameters of such an empirical Padé-type approximant are determined, $g(\theta)$ can be calculated by replacing $I(z)$ in Eq. (3) by the ansatz function (4). One readily obtains

$$g(\theta) = 1/2\pi[1 + (d_1 - d_2)n_1 - d_2 + (1 - d_1 + d_2)n_1 \cos\theta - (1 - d_2 + n_1)\cos(2\theta)]/ [1 + d_1^2 + d_2^2 + 2d_1(1 + d_2)\cos\theta + 2d_2\cos(2\theta)]. \quad (5)$$

In the first step, we have tested the above procedure on numerical data sets of the isothermal magnetization in the case of the linear chain and the mean-field model. The density functions, Eq. (5), emerging from the best fits agree with previous results apart from roundings of the pole occurring for the linear chain and of the steplike change at the upper bound of the gap encountered in the mean-field case [10]. In particular, $g(\theta)$ inherently fulfills the condition [12],

$$\int_0^{\pi} g(\theta)\, d\theta = \frac{1}{2}. \quad (6)$$

In order to test Eq. (5) on real experimental data we have measured the isothermal axial magnetic moment m of the layered antiferromagnet $FeCl_2$, which behaves as a quasi-2D triangular Ising ferromagnet at temperatures well above the 3D ordering temperature, $T_N = 23.7$ K [13,14]. The experiments are carried out on an as-cleft c platelet with thickness $t = 0.5$ mm and area $A = 18$ mm^2 by use of a SQUID magnetometer (Quantum Design MPMS-5S) at temperatures $34 \le T \le 99$ K. The saturation moment, $m_s \approx 4$ kA m^2, is deduced from the high field limit of the m vs H data at $T = 4.5$ K (Fig. 1, dashed line). At this temperature, $FeCl_2$ behaves as a prototypical metamagnet switching from long-range antiferromagnetic into saturated paramagnetic order at $H \approx 0.8$ MA/m. Note that all data have been corrected for demagnetization effects using $H = H_a - Nm$, where H_a is the applied axial magnetic field. N is the demagnetizing factor, which is calculated according to $N = (dm/dH_a)^{-1} \approx$ const for $0.8 < H_a < 1.3$ MA/m, within the coexistence region of the antiferromagnetic and paramagnetic phases [15].

Figure 1 shows the normalized isothermal magnetic moment m/m_s vs H of $FeCl_2$ [13,14] for temperatures $T = 34$, 49, 50, 51, 52, 53, and 99 K. The data are best fitted to Eq. (4). The results of the fitting procedure are indicated in Fig. 1 by full lines and are in detail shown for the extended magnetic field range in the insets (a)–(e) for the temperatures $T_n = 49$ K $+ n\Delta T$, where $\Delta T = 1$ K and $n = 0, 1, \ldots, 4$, respectively.

Figure 2 shows the density functions, $g(\theta)$ which correspond to the magnetization data obtained at $T = 49, \ldots, 53$ K (curves 1–5) and $T = 99$ K (curve 6). They have been calculated via Eq. (5) inserting the fitting parameters n_1, d_1, and d_2 obtained from Eq. (4) and summarized in Table I. The Landé-factor $g = 4.1$ [16] enters z and, hence, Eq. (4), as a fixed parameter. Since the zeros of the partition function of a noninteracting system accumulate at $z = -1$, its density function is given by $g(\theta) = \delta(\theta - \pi)$. The pronounced peak of $g(\theta, T = 99\ \text{K})$ at $\theta = \pi$ (Fig. 2, curve 6) is, hence, in accordance with the limit of weak interaction. With decreasing temperature the maximum value of $g(\theta)$ decreases, while its position shifts towards lower θ-values. For example, at $T = 51$ K (curve 3), $g(\theta)$ is nearly zero for $0 < \theta \lessapprox 0.8$, but exhibits a steep increase with increasing θ, which yields a maximum of $dg/d\theta$ at $\theta = 1.5$.

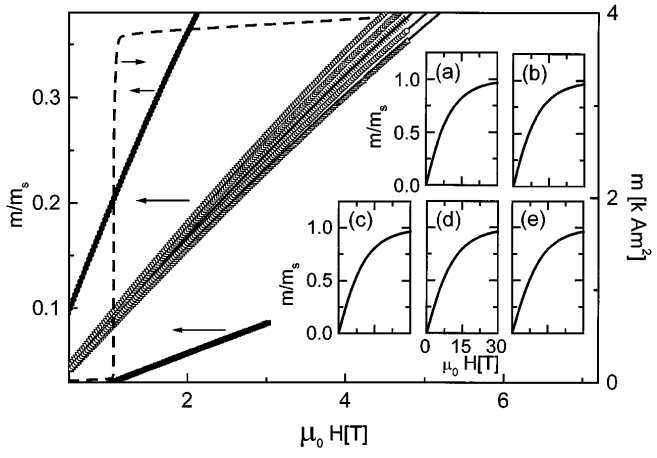

FIG. 1. m/m_s vs H of $FeCl_2$ for temperatures $T = 34$, 49, 50, 51, 52, 53, and 99 K (solid circles, down triangles, open squares, crosses, open circles, up triangles, and solid squares, respectively) and $T = 4.5$ K (dashed line). Results of the best fits of Eq. (4) to the data at $T = 49, \ldots, 53$ K are indicated by full lines and in detail shown within the insets [(a),(b), ..., (e), respectively].

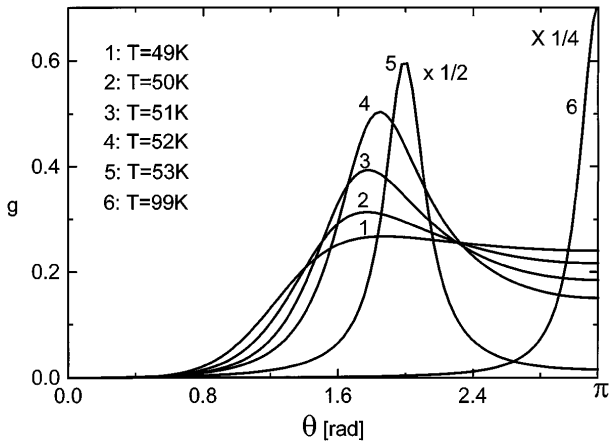

FIG. 2. LY-zero density function $g(\theta)$ for $T = 49$, $50, \ldots, 53$ K (curves 1–5, respectively) and $T = 99$ K (curve 6). Data of curve 5 and 6 are scaled by factors $\frac{1}{2}$ and $\frac{1}{4}$, respectively.

TABLE 1. Best-fit parameters n_1, d_1, and d_2 of Eq. (4) to the m/m_s vs H data partially displayed in Fig. 1; $J/k_B = -(T/12)\ln[(d_1 - n_1)/2]$; and quality parameter χ^2, which measures the sum of the squares of the deviations of Eq. (4) from the respective data points normalized to the degrees of freedom.

T [K]	n_1	d_1	d_2	J/k_B [K]	χ^2
34	−1.5583	−1.07621	0.44795	4.031	2.45×10^{-7}
35	−1.62526	−1.09583	0.42893	3.877	4.66×10^{-7}
36	−1.60725	−1.04905	0.41056	3.829	6.26×10^{-7}
49	−1.22375	−0.33542	0.28636	3.314	2.86×10^{-7}
50	−1.00352	−0.12235	0.35496	3.415	1.84×10^{-7}
51	−0.79428	0.07411	0.44338	3.546	1.79×10^{-8}
52	−0.58248	0.28942	0.52122	3.598	6.10×10^{-8}
53	−0.10146	0.71108	0.74829	3.978	2.28×10^{-8}
99	−0.41602	1.50348	0.54979	0.339	5.90×10^{-9}

The pronounced peak at $\theta = 1.8$ is followed by a smooth decay into the constant value $g(\theta = \pi) = 0.19$. This behavior bears similarity with the θ-dependence of the density function of the square lattice, which was theoretically determined at $T = 6T_c$ [10]. The observed steep increase of $g(\theta)$ indicates the upper bound of the gap, $g(\theta) = 0$ for $0 < \theta < \theta_g$, while the pronounced peak in curve 3 reflects the smeared singularity at $\theta = \theta_g$. This smearing originates from the truncation of the Padé-type expansion used in Eq. (4). This was clearly evidenced in the case of the linear chain, whose exactly known [10] singularity becomes rounded within our approach (see above). In addition, however, one has to take into account the dependence of $m(H)$ on the details of the lattice structure. Hence, one might also expect qualitative differences between the underlying density functions of the square and the triangular lattice. Tentatively, this might be at the origin of the discrepancy between the steep decay of $g(\theta \to \pi)$ in the case of the square lattice [10] and its virtual absence in the case of the triangular lattice (Fig. 2).

The validity of our procedure yielding the density function, $g(\theta)$, from experimental magnetization data, $m(H)$, is determined by a comparison of the magnetic specific heat, $c(H)$, as deduced from either $g(\theta)$ or $m(H)$. Both results are shown in Fig. 3 by the functions $c(H)$ and $\Delta c(H)$, respectively.

The function $\Delta c = [c(H) - c(H = 0)]/m_s$ is calculated from the fitting results shown in Fig. 1 [inset (a)–(e)] according to

$$\Delta c = T \int_0^H \partial^2(m/m_s)/\partial T^2 \, dH'. \tag{7}$$

Equation (7) is derived from Maxwell's relation $\partial M/\partial T = \partial S/\partial H$ [17,18]. The second order derivative which enters the integral is approximately given by $\partial^2 m/\partial T^2 = (1/12)[-m(T = 49\ \mathrm{K}) + 16m(50\ \mathrm{K}) - 30m(51\ \mathrm{K}) + 16m(52\ \mathrm{K}) - m(53\ \mathrm{K})]\mathrm{K}^{-2}$ [9].

The alternative method to obtain $c(H)$ utilizes the density function $g(\theta)$ in conjunction with the magnetic free-energy function [1],

$$F/Ng\mu_B S = -\mu_0 H - (k_B T/g\mu_B S) \times \int_0^\pi g(\theta)\ln(z^2 - 2z\cos\theta + 1)\, d\theta, \tag{8}$$

where $N = m_s/g\mu_B S$ is the number of spins. By inserting the $g(\theta)$ functions shown in Fig. 2 and the respective $z(T, H)$ values one obtains F vs H curves, which are displayed in Fig. 4 for $T = 49$, 50, 51, 52, and 53 K (curves 1–5, respectively). From these functions the magnetic entropy, s, and the specific heat, c, is calculated by numerical derivation as shown for $T = 51$ K in Fig. 4 (inset) and Fig. 3 (open circles), respectively. It is seen that, apart from small deviations which originate from errors of the numerical integration, both curves $\Delta c(H)$ and $c(H)$ yield identical results, where $c(H = 0) = -\Delta c(H \to \infty)$ as expected.

Since the curvature of m/m_s vs H is weak in the available field range of the magnetometer, the extrapolation of the fitting results into the high field regime is risky and has to be checked separately. Therefore we calculate the leading term of the high field series of $f(z)$, Eq. (4),

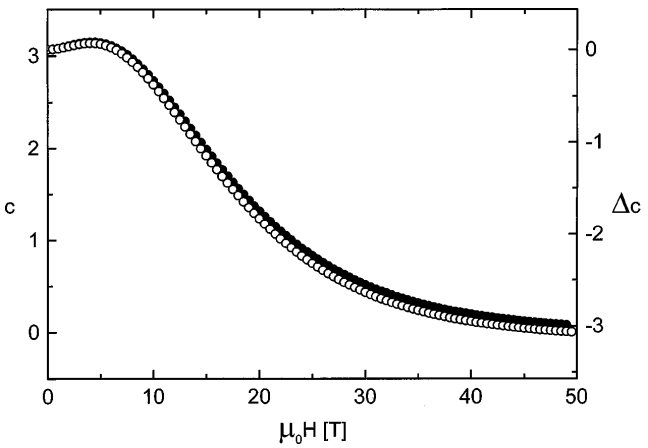

FIG. 3. Field dependence of c (open circles) and Δc (solid circles) calculated from $g(\theta)$ and by use of Maxwell's relation, respectively.

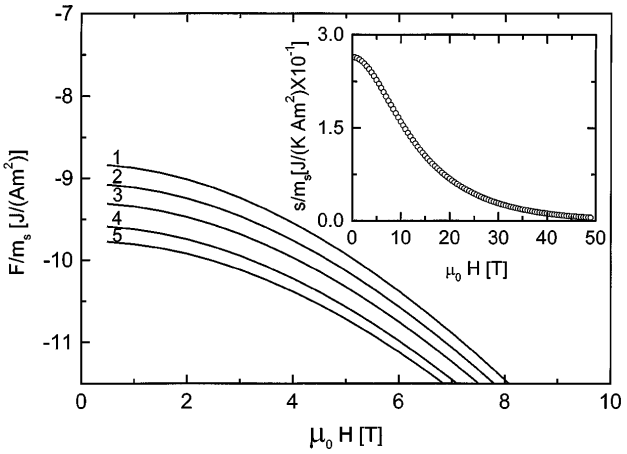

FIG. 4. Field dependence of the free energy calculated from $g(\theta)$ at $T = 49, \ldots, 53$ K (curves 1–5, respectively). The inset shows the field dependence of the entropy at $T = 51$ K calculated from the free-energy curves 1, 2, 4, and 5 by numerical derivation.

which reads $f(z) = 1 - (d_1 - n_1)z + \mathrm{O}[z^2]$. Comparison with the theoretical expansion of the magnetization of the 2D Ising ferromagnet on a triangular lattice [11] yields $u^3 = (1/2)(d_1 - n_1)$, where u is given by $u = \exp(-4J/k_{\mathrm{B}}T)$. Hence, the ferromagnetic nearest neighbor in-plane exchange constant of $FeCl_2$ is related to the fitting parameters n_1 and d_1 according to $J/k_{\mathrm{B}} = -(T/12)\ln[(d_1 - n_1)/2]$. The average value of the exchange constant yields $J/k_{\mathrm{B}} = 3.7$ K for $34 \leq T \leq 53$ K. Within an error of $\approx 6\%$ this is in accordance with the value $J/k_{\mathrm{B}} = 3.94$ K which has been determined from magnon dispersion data of inelastic neutron scattering investigations on $FeCl_2$ [14]. Disappointingly, the value from the data at $T = 99$ K, $J/k_{\mathrm{B}} = 0.339$, deviates from the experimental one by 1 order of magnitude. Presumably this is due to the finite value of the single-ion anisotropy of $FeCl_2$ [14], which violates the condition of Ising-type symmetry at high temperatures.

In conclusion, it has been shown for the first time, that the LY-zero density can be determined experimentally with high accuracy from the field dependence of the isothermal magnetization data, $m(H)$, of a quasi-2D Ising ferromagnet. In accordance with theoretical predictions [1] and model calculations [1–7,10] $g(\theta)$ exhibits a gap in the low-θ region, which shrinks upon lowering the temperature towards the phase transition instability. The resulting density functions are used to calculate the field dependencies of the magnetic free energy, the entropy, and the specific heat. The latter quantity is alternatively calculated from $m(H)$ by utilizing Maxwell's relation. The results of both methods are in nearly perfect agreement.

It will be interesting to perform high field magnetization measurements in the regime of strong curvature of the m vs H dependencies. These data will require Padé-type approximants, which contain relevant additional free parameters. Such higher order approximants are expected to reduce the smearing of possible singularities and steps contained in the density functions. Furthermore, investigations on Ising ferromagnets in other dimensions, $D = 1$ and 3, seem desirable in order to reveal pertinent differences [1] with the $D = 2$ case considered in this Letter. Finally, it will be a challenging future task to determine the ill-known symmetries of the zero distribution in the case of antiferromagnetic systems [5,7] in a similar way as has been done here on Ising ferromagnets.

I thank W. Kleemann for very fruitful discussions.

[1] T. D. Lee and C. N. Yang, Phys. Rev. **87**, 410 (1952).
[2] S. Katsura, Y. Abe, and K. Ohkohchi, J. Phys. Soc. Jpn. **29**, 845 (1970).
[3] V. Matveev and R. Shrock, Phys. Lett. A **215**, 271 (1996).
[4] S. Ono, Y. Karaki, M. Suzuki, and C. Kawabata, J. Phys. Soc. Jpn. **25**, 54 (1968).
[5] M. Suzuki, C. Kawabata, S. Ono, Y. Karaki, and M. Ikeda, J. Phys. Soc. Jpn. **29**, 837 (1970).
[6] C. Kawabata and M. Suzuki, J. Phys. Soc. Jpn. **28**, 16 (1970).
[7] S. Katsura, Y. Abe, and M. Yamamoto, J. Phys. Soc. Jpn. **30**, 347 (1971).
[8] This was originally pointed out by LY, but is more easily seen using the concept of Z transformations which is briefly introduced here. Using the symmetry $I(\tilde{z} = 1/z) = -I(z)$, since $m(-H) = -m(H)$, the normalization $\int_0^\pi g(\theta)d\theta = \frac{1}{2}$, and the representation $\sum_{n=0}^{\infty}\cos(n\theta)\tilde{z}^{-n} = \tilde{z}(\tilde{z} - \cos\theta)/(\tilde{z}^2 - 2\tilde{z}\cos\theta + 1)$ of the Z transform of $\cos(n\theta)$, one obtains $I = 1 + 2\pi\sum_{n=1}^{\infty} g_n z^n$, where $g_n = (2/\pi)\int_0^\pi g(\theta)\cos(n\theta)\,d\theta$ is the nth coefficient of the cosine Fourier series of $g(\theta)$. If $-(I + 1)/2\pi$ can be approximated by the ratio $P(\tilde{z})/Q(\tilde{z})$ of two polynomials P and Q, the coefficients are determined as $g_n = \sum_{i=1}^{k}\mathrm{Res}_{\tilde{z}_i}[P(\tilde{z})/Q(\tilde{z})\tilde{z}^{n-1}]$ [9], where $\tilde{z}_i$ is the ith zero of Q and $\mathrm{Res}_{\tilde{z}_i}$ is the residue at $\tilde{z} = \tilde{z}_i$. Note that the convergence of the Fourier series of $g(\theta)$ requires $|\tilde{z}_i| < 1$.
[9] I. N. Bronstein and K. A. Semendjajew, *Taschenbuch der Mathematik* (Harri Deutsch, Frankfurt/Main, 1989), 24th ed.
[10] P. J. Kortman and R. B. Griffiths, Phys. Rev. Lett. **27**, 1439 (1971).
[11] M. F. Sykes, J. W. Essam, and D. S. Gaunt, J. Math. Phys. **6**, 283 (1965).
[12] Every function g, which is constructed according to Eq. (3) from an arbitrary function I obeying $I(z = 1) = 0$ and $I(z = 0) = 1$, fulfills Eq. (2).
[13] L. J. De Jongh and A. R. Miedema, Adv. Phys. **23**, 1 (1974).
[14] R. Birgeneau, W. B. Yelon, E. Cohen, and J. Makovsky, Phys. Rev. B **5**, 2607 (1972).
[15] J. F. Dillon, E. Y. Chen, and H. J. Guggenheim, Phys. Rev. B **18**, 377 (1978).
[16] D. Bertrand, F. Bensamka, A. R. Fert, J. Gelard, J. P. Redoulès, and S. Legrand, J. Phys. C **17**, 1725 (1984).
[17] H. Mitamura, T. Sakakibara, G. Kido, and T. Goto, J. Phys. Soc. Jpn. **64**, 3459 (1995).
[18] O. Petracic, Ch. Binek, W. Kleemann, U. Neuhausen, and H. Lueken, Phys. Rev. B **57**, R11 051 (1998).